A FINITE-DIFFERENCE SIMULATION OF MULTI-MODE LAMB WAVES IN ALUMINIUM SHEET WITH EXPERIMENTAL VERIFICATION USING LASER BASED ULTRASONIC GENERATION

Vajradehi B. Yadav, T. Pramila*, V. Raghuram and N. N. Kishore

Indian Institute of Technology Kanpur, Kanpur, India
*Christ Church College, Kanpur, India

Abstract

Laser based ultrasonics is a fast growing technique for Non-destructive Evaluation (NDE) of materials. However, the complexity due to simultaneous multi-mode generation of laser-generated signals restricts its utility. This paper describes a simple finite difference method (FDM) to simulate multiple modes of Lamb waves occurring simultaneously in thin Aluminium sheet generated using an excitation pulse modeled on Nd^+ YAG laser pulse. The simulation is used to predict time domain histories of vertical displacements at various points on the sheet. The wavelet transforms of these simulated signals are obtained and compared with the wavelet transforms of experimental signals. The experimental signals are obtained using a pulsed Nd^+ YAG laser and detected by a He-Ne heterodyne laser interferometer. Experimental results show good agreement with simulated signals.

1. Introduction

Lamb waves arise from a coupling between shear and longitudinal waves reflected at the top and bottom of plate surface [1]. Lamb waves are waves of plane strain that occurs in thin plate, and the traction force must vanish on the upper and lower surfaces of plate. Propagation properties of these waves depend on frequency of vibration and thickness of plate [2]. Lamb wave theory is fully documented in a number of textbooks [3-4]. Structural flaws such as corrosion and fatigue cracks represent changes in effective thickness and local material properties, and therefore measurement of variations in Lamb wave propagation can be employed to assess the integrity of plate structures [5]. Worlton [6] provided experimental confirmation of Lamb waves at megacycle frequencies. Cheng et.al. [7] have presented the study of laser-generated Lamb waves in orthotropic plates. Tan et al. [8] have discussed the experimental evaluation of delaminations in composite plates by the use of Lamb waves.

Explicit finite-difference (FD) schemes were the first numerical methods to be applied to solve propagating stress-wave problems [9-10]. Balasubramanyam [11] explained a finite-difference method to simulate S_0 and A_1 Lamb wave modes in plane metal sheets with experimental verification using water-coupled transducers. Harker [12] used finite difference scheme for scattering of waves using impedance mismatch method.

2. The Free Plate Problem

The classical problem of Lamb wave propagation is associated with wave motion in a stress-free plate. The geometry of the free plate problem is illustrated in Fig. 1.

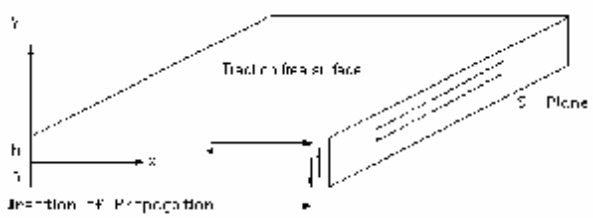

Figure 1*: Geometry of Schematic of traction-free plate.*

The equation of motion for particle displacement u for any continuous medium is given by Navier's equation as

$$(l + m)u_{j,ij} + mu_{i,jj} + rf_i = r\ddot{u}_i \quad (1)$$

where l and m are Lame's constants, r is the density of material and f is the body force . The surfaces at y=h and y= -h are considered traction-

free. Plane strain condition is assumed which eliminates the movement in z direction and hence dependence of displacement on z .Let u and v be the displacements in x and y direction respectively. Depending on the particle displacement (symmetric or anti-symmetric) about the centre line of plate (about x-axis) there are two different modes of vibration called symmetric and anti-symmetric modes. The two different modes of Lamb waves are shown schematically in Fig. 2. Depending on their cut-off frequencies, the different modes will be present in the Lamb wave.

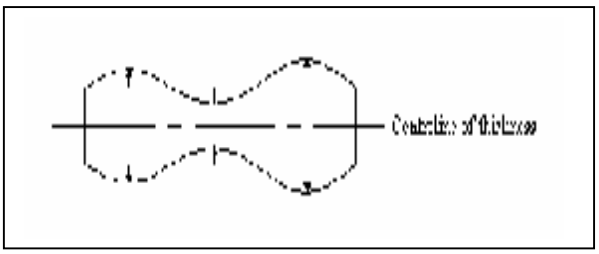

Symmetric mode (S)

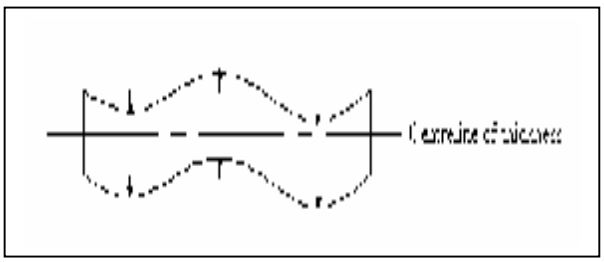

Anti-symmetric mode (A)

Figure 2: *Lamb wave modes*

For the conditions of plane strain and traction-free surfaces, the governing equation (1) reduces in the set of two equations called Rayleigh-Lamb frequency equations. They are given by,

$$\frac{\tan(qh)}{\tan(ph)} = -\frac{4k^2 pq}{\left(q^2 - k^2\right)^2}, \quad \text{for symmetric modes}$$

$$\frac{\tan(qh)}{\tan(ph)} = -\frac{\left(q^2 - k^2\right)^2}{4k^2 pq}, \quad \text{for anti-symmetric modes}$$

where, $p^2 = \frac{w^2}{c_L^2} - k^2$ and $q^2 = \frac{w^2}{c_T^2} - k^2$

h is half plate thickness, w is circular frequency of vibration, c_L, c_T are longitudinal and shear wave velocities for the medium and k is wave number. Lamb wave is the group of waves that get reflected from upper and lower surface of plate and recombine into a packet at later length. So, Lamb wave travels with the group velocity. This is the speed with which the energy in Lamb wave propagates. Therefore, group velocity is the characteristic of Lamb waves that mainly depends on frequency of vibration as well as thickness of plate. This dependence gives rise to the dispersive nature of Lamb waves. The graph of group velocities verses different frequency-thickness products is called as dispersion curves. Typical dispersion curves for lowest symmetric and anti-symmetric Lamb wave modes for Aluminium are shown in Fig. 3. It can be seen from dispersion curves that the group velocities change as the frequency-thickness product increases.

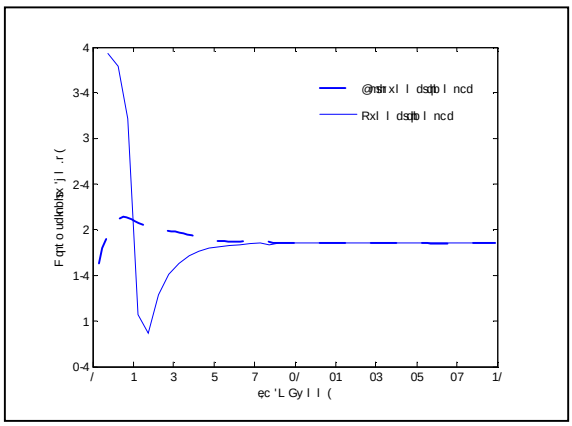

Figure 3: *Dispersion curves for Aluminum*

3. Lamb wave in Finite Difference form

FD methods have been implemented successfully in the field of seismology for elastic waves [13]. In FD methods realistic pulse shapes can be used as an excitation. The output of FD calculations corresponds to the time trace on the oscilloscope of NDE operator. For a plain strain problem equation (1) reduces to

$$u_{tt} = c_T^2(u_{xx} + u_{yy}) + (c_L^2 - c_T^2)(u_{xx} + v_{xy}) \qquad (2)$$

$$v_{tt} = c_T^2(v_{xx} + v_{yy}) + (c_L^2 - c_T^2)(u_{xy} + v_{yy}) \qquad (3)$$

where

$$\frac{\partial^2 u}{\partial x^2} = u_{xx} \qquad \frac{\partial^2 u}{\partial y^2} = u_{yy} \qquad \frac{\partial^2 u}{\partial t^2} = u_{tt} \qquad (4)$$

Similar conventions are used for v. The longitudinal wave speed and shear wave speed is given by,

$$c_L^2 = \frac{l + 2m}{r} \qquad c_T^2 = \frac{m}{r} \qquad (5)$$

u and v are defined over uniform Cartesian mesh of interval h in both x and y directions and at time intervals Δt . In x-y plane u and v can be defined as

$$u(m, n, l) = u(mh, nh, l\Delta t) \qquad (6)$$

and a similar relation for v.

According to second order difference form u can be expressed as

$$u_{tt}(m,n,l)=\frac{1}{\Delta t^2}[u(m,n,l+1)-2u(m,n,l)+u(m,n,l-1)] \quad (7)$$

$$u_{xx}(m,n,l)=\frac{1}{h^2}[u(m+1,n,l)-2u(m,n,l)+u(m-1,n,l)] \quad (8)$$

$$u_{xy}(m,n,l)=\frac{1}{4h^2}\begin{bmatrix}u(m+1,n+1,l)-u(m+1,n-1,l)\\-u(m-1,n+1,l)+u(m-1,n-1,l)\end{bmatrix} \quad (9)$$

Substituting these equations in equations (2 and 3) and defining $\frac{\Delta t}{h}=b$ we get

$$\begin{aligned}&u(m,n,l+1)=2u(m,n,l)(1-b^2c_L^2+b^2c_T^2)\\&-u(m,n,l-1)+b^2c_L^2(u(m+1,n,l)+u(m-1,n,l))\\&+b^2c_T^2(u(m,n+1,l)+u(m,n-1,l))\\&+\frac{b^2(c_L^2-c_T^2)}{4}(v(m+1,n+1,l)-v(m+1,n-1,l)\\&-v(m-1,n+1,l)+v(m-1,n-1,l))\end{aligned} \quad (10)$$

Similar relations can be written for v.
The above system was investigated by Alterman [14], where he gave following stability condition

$$\beta \le 1/\sqrt{(c_L^2+c_T^2)} \quad (11)$$

Condition of stability states that the signal will not be able to propagate across one mesh spacing in less than one time step. Matlab code is developed for FD algorithm. In the code u and v are defined as three dimensional matrix u (M, N, l). M is the number of grid points on x-axis and N is the number of grid points on y-axis. At each grid point, at the beginning of time step $l\Delta t$, the displacements at times $(l-1)\Delta t$ and $(l-2)\Delta t$ are known and the displacements at time $l\Delta t$ are calculated using relations for u and v.

3.1. Boundary conditions

Fundamental difference between bulk wave and Lamb wave is that Lamb wave satisfies stress free boundary condition at top and bottom surface of plate. For stress-free boundaries, the finite difference equations are expressed in one-sided form for derivatives normal to the boundary and in centered form for tangential derivatives [12,13]. This method gave a stability condition in code, which is simple to implement. The application of the method gives the "pseudo node" formulation, in which a row of points is added just outside the free surface, and the displacements of those points are adjusted to give zero stress at the boundaries.

Stress free boundary condition is given as

$$\begin{aligned}&(c_L^2-2c_T^2)u_x+c_L^2v_y=\frac{s_{yy}}{r}=0\\&c_T^2(v_x+u_y)=\frac{s_{xy}}{r}=0\end{aligned} \quad (12)$$

The governing equations for evaluating displacements u and v at points on the boundary are given as

$$\begin{aligned}&(c_L^2-2c_T^2)[u(m+1,n,2)-u(m-1,n,2)]\\&+2c_L^2[v(m,n,2)-v(m,n-1,2)]=0\\&2[u(m,n,2)-u(m,n-1,2)]\\&+v(m+1,n,2)-v(m-1,n,2)=0\end{aligned} \quad (13)$$

Other boundary conditions are evaluated as given in Harker [12].

3.2. Input parameters for simulation

Simulation is done for Aluminum plate for thickness (d in Fig. 4) 3.4 mm and 8 mm. The material properties for Aluminum $c_L = 6230$ m/s and $c_T = 3130$ are taken from Rose [2]. The grid size is chosen as 0.2 mm and time step 0.02 ms. Detector (point R) is moved over plate to detect the signal at various distances.

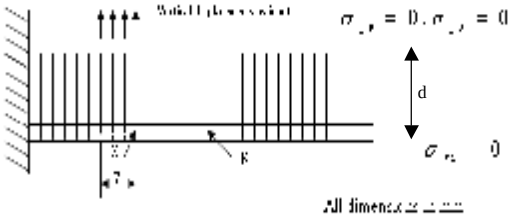

Figure 4: *Simulation Model*

Input normal disturbances are given over 7 mm length and across the thickness of plate in form of tone burst represented by following relation as given in reference [15].

$$u(t)=\begin{cases}u_0\sin(wt).\left\{\sin(\frac{wt}{10})\right\}^2 & t<\frac{10p}{w}\\0 & otherwise\end{cases} \quad (14)$$

Simulation results are presented as time history. A time history is the graph of the displacement of a particular point on the grid as a function of time. This corresponds to an experimental signal taken by oscilloscope

4. Experimental Details

The Laser based ultrasonic (LBU) setup consists of an Nd: YAG pulsed laser to generate ultrasonic Lamb waves and a Heterodyne laser interferometer to detect the transmitted acoustic signal through the material. The set-up utilizes a Yokogawa DL1740 (four channel, one GSa/sec, 500 MHz) Digital Storage Oscilloscope. The schematic layout is shown in Fig. 5. The scanning is done manually using an XY translator mounted on an Optical Test Bench.

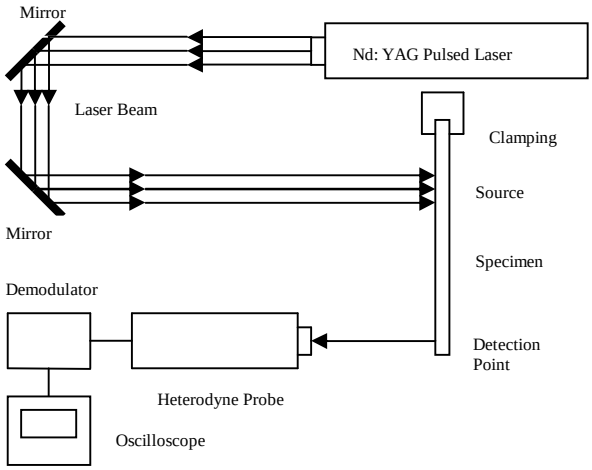

Figure 5: *Schematic of experimental set-up*

Two Aluminium plates of thickness 3.4 mm and 8 mm are used as a specimen to generate Lamb waves. The laser power is kept at 200 mJ. A precise calibration of heterodyne interferometer is done prior to the experiment. Wavelet transforms are obtained using Morlet mother wavelet. These wavelet transforms are compared with the wavelet transform of simulated signals. The arrival times of different frequency components are extracted from the wavelet transforms. Knowing the arrival times, group velocities at a particular frequency are calculated and the values are compared with those obtained from the simulation.

5. Results and Discussion

As the recorded signals are expected to contain various frequencies, the wavelet transform of each signal is used to analyze the arrival time for different frequencies. The fundamental idea behind wavelets is to analyze according to scale. Wavelet transform of signal obtained for 8mm plate (Figs. 6 and 7) shows 3 windows. Window at the top shows the signal whose wavelet is to be taken. Middle window shows the three-dimensional plot in which x-axis corresponds to time, y-axis corresponds to frequency according to scale, and z-axis shows the variation of amplitude. The variation in amplitude is depicted in the Figs. (6 and 7) with the help of different colors with red corresponding to maximum intensity. Last window gives temporal distribution of signal at frequency corresponding to a given scale.

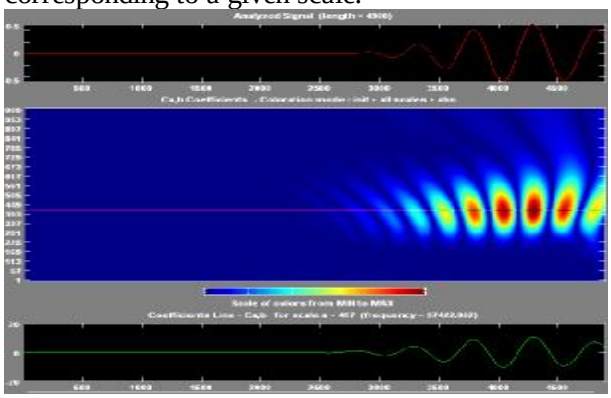

Figure 6: *Wavelet transform of signal of 8mm plate at 200 mm separation (Simulated)*

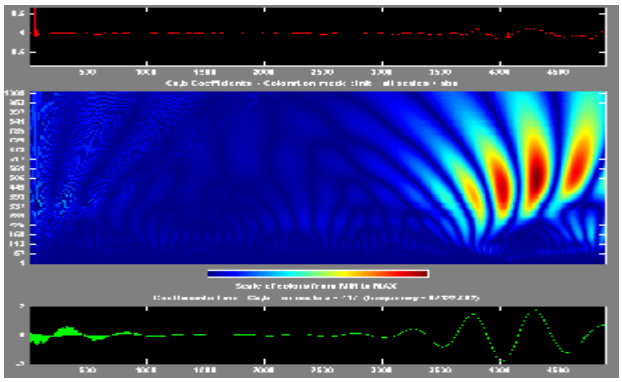

Figure 7: *Wavelet transform of signal of 8 mm plate at 200 mm separation (Experimental)*

From both the wavelets (Figs. 6 and 7) one can notice the experimental signal contains the intensity (color) distribution same as that of the output signal from simulation when a tone burst is used as input in the simulation. According to Harker [12], when normal stress is given as input to plate the symmetric modes will have less probability of generation. As the generation of waves is through normal disturbances in experimental condition, only A_0 mode is obtained with greater intensity. In simulation also the normal displacements are given as input to plate over 7 mm length and a sampling period of 20 ns is used for the evaluation of both wavelet transforms. The mother wavelet used is Morlet whose center frequency is 0.8125 Hz. From Figs. 6 and 7, the arrival time for A_0 mode for source to detector distance of 200 mm by simulation is coming out to be $62\,ms$ and by experiments it is coming out to be $68\,ms$ at 97 kHz. The velocity by simulation is 3.22 km/s and by experiment it is coming out to be

2.94 km/s. The velocity for A_0 mode from dispersion curve is 3.06 km/s. The coefficients of wavelets are stored in matrix form for further analysis.

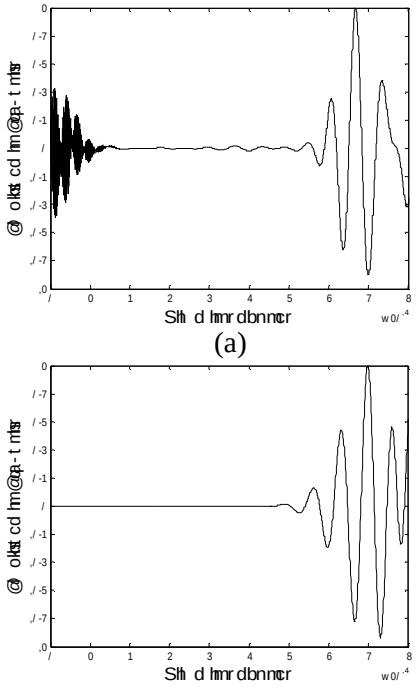

(a)

(b)

Figure 8: (a) *Experimental Signal* (b) *Simulated Signal at 253 kHz obtained from wavelet transform (source to detector distance 200 mm, plate thickness 8mm)*

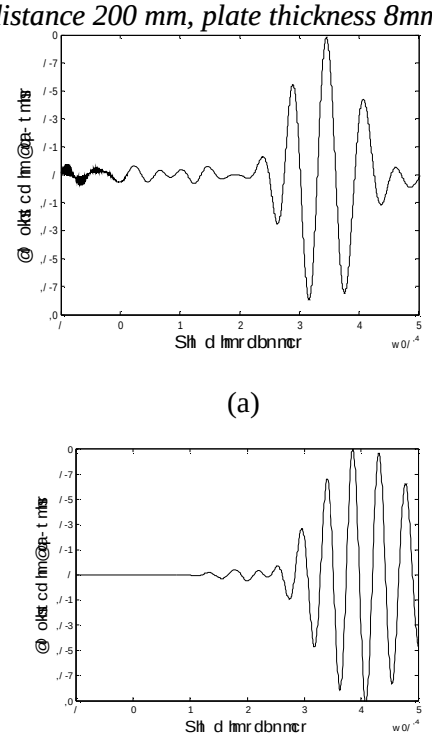

(a)

(b)

Figure 9**:** (a) *Experimental Signal* (b) *Simulated Signal at 203 kHz obtained from wavelet transform (source to detector distance, 85mm, plate thickness 3.4 mm)*

At a particular point on the y-axis i.e. when the scale fixed, the plot between x and z-*axes* will give temporal distribution of the signal at particular frequency. The experimental and simulated signals obtained from wavelet transforms at 253 kHz for 8mm plate and at 203 kHz for 3.4mm plate are shown in Figs. 8 and 9 respectively. The disturbances seen near zero microseconds in Figs. 8(a) and 9(a) are due to trigger characteristic of the laser pulse.

Table 1: Comparison between experimental and simulation result

Frequency-thickness (*fd*) (MHz-mm)	Group velocity of A_0 mode by simulation (km/s)	Group velocity of A_0 mode by experiment (km/s)
2.024	3.22	2.94
0.692	2.42	2.65

In Fig. 9 the presence of S_0 mode can be seen preceding A_0 mode with smaller amplitude as expected. Table 1 shows the comparison between group velocities obtained from experiments and simulation. The results are evidently in good agreement.

5.1 Dependence of mode amplitude on frequency

From Fig. 10 shows the time history of the signal obtained from the wavelet transform of the experimental signal on 3.4 mm plate with source-detector separation of 85mm. In this figure both S_0 and A_0 modes can be seen to appear simultaneously. These modes are identified with the help of their group velocities

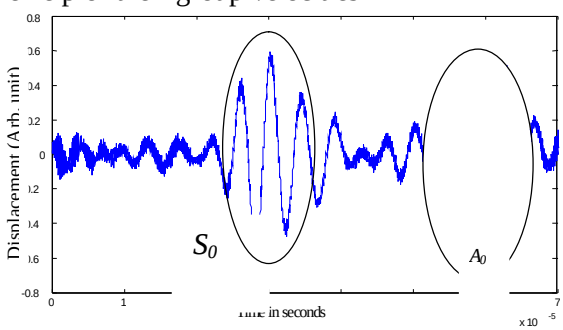

Figure 10: *Time history of signal at 251 KHz on 3.4 mm plate(experimental).*

Figure 11 shows result of FEM simulation done by Nieuwenhuis[15]. The encircled region shows the matching between the amplitudes of two modes at frequency of 250 kHz

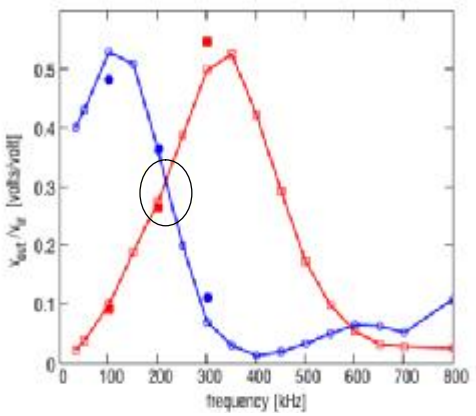

Figure 11: *Simulated results for dependence of mode amplitude on excitation frequency [15*].

Figure 12 (a and b) shows the temporal distribution (obtained by wavelet) of the experimental results conducted on 3.4 mm thick plate at source-detector separation distance of 85mm. One can obviously see the amplitude of the S_0 mode to be equal to that of A_0 mode around 250 kHz while it is much less at 120 kHz in agreement with the results shown in Fig. 11

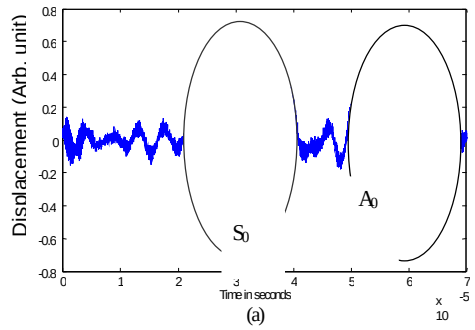

Figure 12: *Signals at separation distance 85 mm (a) at 231 kHz, (b) at 120 kHz.*

Conclusions:

In the present work the results of FDM simulation of Lamb waves in Aluminium plates of different thickness and their correlation with Laser generated lamb waves are presented. Wavelet Transforms are used to study this correlation. The work presented in this paper clearly brings out the utility of wavelet transforms in the analysis of complex signals as well as in confirming the accuracy of any simulation work. The variation of amplitude of different Lamb wave modes with frequency is studied with the help of wavelet transforms of the experimental signals and a good correlation between the experimental and simulation results is observed.

6 References:

[1] Viktorov I. A, *Rayleigh and Lamb wave. Physical Theory and Applications,*: Plenum, New York 1970.

[2] Rose, J. L, *Ultrasonic waves in solid media*, The Pennsylvania State University, Cambridge University Press, 1999.

[3] Graff, K.F., *Wave Motions in Elastic Solids*, Dover Publications Inc., 1991.

[4] Achenbach J. D. *Wave propagation in elastic solids*, North Holland publishing company,1973.

[5] Alleyene, D. N, Cawley, P., "The interaction of lamb waves with defects*", IEEE Trans. Ultrason. Ferroelectr. Freq. Control*, 39 (3) 381-97, 1992

[6] Worlton D. C. Ultrasonic testing with Lamb waves *Non-dest. Testing,(*15) 218–22, 1957.

[7] Cheng J. C., "Theory of laser-generated transient Lamb waves in orthotropic plates", *J. Phys. D: Appl. Phys.*, (29) 1857-67, 1996.

[8] Tan K. S., Guo N., Wong B. S., "Experimental evaluation of delaminations in composite plates by the use of Lamb waves", *Composite Science and Technology*, 53 (2) 404-11, 1994.

[9] Bertholf L. D., "Numerical solutions to two-dimensional elastic wave propagation in finite bars", *J. Appl. Mech. (*34) 725–734, 1967.

[10] Alterman Z., "Finite difference solutions to geophysical problems" *J. Phys. Earth,* (16) 113–128, 1968.

[11] Balasubramanyamy R., Quinneyz D., Challisy R E and Toddy, C. P. D., "A finite-difference simulation of ultrasonic Lamb waves in metal sheets with experimental verification", *J. Phys. D: Appl. Phys.* (29) 147–155, 1996.

[12] Harker A. H., "Numerical modelling of the scattering elastic waves in plates", *J. Non-dest. Eval.* (4) 89–106, 1984.

[13] Alterman, Z. S, and Loewenthal, D, "Seismic waves in a quarter and three quarter plane" *Geophys. J. Roy. Astron. Soc, (*20):101,1970.

[14] Alterman, Z, and Loewenthal, D., "Computer generated seismograms", *Methods in Computational Physics, V*ol 12, ed Adder, B *et al.,*: Academic Press, New York, 1972

[15] Nieuwenhuis J.H., Neumann J. J., Greve D.W., and Oppenheim I.J. ''Simulation and Testing of Transducers for Lamb wave Generation." *IMAC-XXIII Conference on Structural Dynamics, Society for Experimental Mechanics, Orlando, February 2005.*

A FINITE-DIFFERENCE SIMULATION OF MULTI-MODE LAMB WAVES IN ALUMINIUM SHEET WITH EXPERIMENTAL VERIFICATION USING LASER BASED ULTRASONIC GENERATION

Vajradehi B. Yadav, T. Pramila*, V. Raghuram and N. N. Kishore

Indian Institute of Technology Kanpur, Kanpur, India
*Christ Church College, Kanpur, India

Abstract

Laser based ultrasonics is a fast growing technique for Non-destructive Evaluation (NDE) of materials. However, the complexity due to simultaneous multi-mode generation of laser-generated signals restricts its utility. This paper describes a simple finite difference method (FDM) to simulate multiple modes of Lamb waves occurring simultaneously in thin Aluminium sheet generated using an excitation pulse modeled on Nd^+ YAG laser pulse. The simulation is used to predict time domain histories of vertical displacements at various points on the sheet. The wavelet transforms of these simulated signals are obtained and compared with the wavelet transforms of experimental signals. The experimental signals are obtained using a pulsed Nd^+ YAG laser and detected by a He-Ne heterodyne laser interferometer. Experimental results show good agreement with simulated signals.

1. Introduction

Lamb waves arise from a coupling between shear and longitudinal waves reflected at the top and bottom of plate surface [1]. Lamb waves are waves of plane strain that occurs in thin plate, and the traction force must vanish on the upper and lower surfaces of plate. Propagation properties of these waves depend on frequency of vibration and thickness of plate [2]. Lamb wave theory is fully documented in a number of textbooks [3-4]. Structural flaws such as corrosion and fatigue cracks represent changes in effective thickness and local material properties, and therefore measurement of variations in Lamb wave propagation can be employed to assess the integrity of plate structures [5]. Worlton [6] provided experimental confirmation of Lamb waves at megacycle frequencies. Cheng et.al. [7] have presented the study of laser-generated Lamb waves in orthotropic plates. Tan et al. [8] have discussed the experimental evaluation of delaminations in composite plates by the use of Lamb waves.

Explicit finite-difference (FD) schemes were the first numerical methods to be applied to solve propagating stress-wave problems [9-10]. Balasubramanyam [11] explained a finite-difference method to simulate S_0 and A_1 Lamb wave modes in plane metal sheets with experimental verification using water-coupled transducers. Harker [12] used finite difference scheme for scattering of waves using impedance mismatch method.

2. The Free Plate Problem

The classical problem of Lamb wave propagation is associated with wave motion in a stress-free plate. The geometry of the free plate problem is illustrated in Fig. 1.

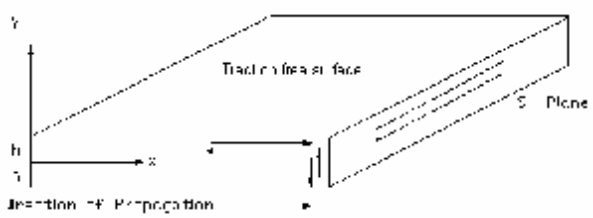

Figure 1*: Geometry of Schematic of traction-free plate.*

The equation of motion for particle displacement u for any continuous medium is given by Navier's equation as

$$(l + m)u_{j,ij} + mu_{i,jj} + rf_i = r\ddot{u}_i \quad (1)$$

where l and m are Lame's constants, r is the density of material and f is the body force . The surfaces at y=h and y= -h are considered traction-

free. Plane strain condition is assumed which eliminates the movement in z direction and hence dependence of displacement on z .Let u and v be the displacements in x and y direction respectively. Depending on the particle displacement (symmetric or anti-symmetric) about the centre line of plate (about x-axis) there are two different modes of vibration called symmetric and anti-symmetric modes. The two different modes of Lamb waves are shown schematically in Fig. 2. Depending on their cut-off frequencies, the different modes will be present in the Lamb wave.

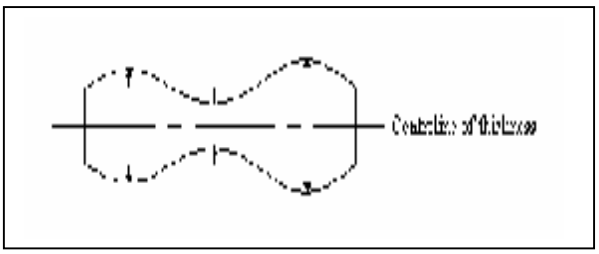

Symmetric mode (S)

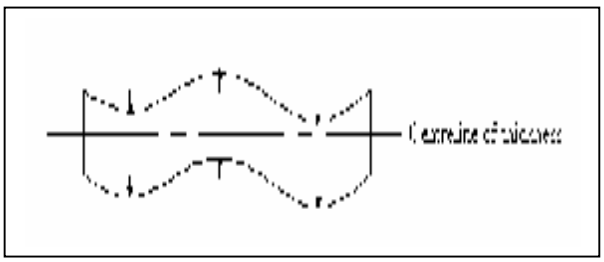

Anti-symmetric mode (A)

Figure 2: *Lamb wave modes*

For the conditions of plane strain and traction-free surfaces, the governing equation (1) reduces in the set of two equations called Rayleigh-Lamb frequency equations. They are given by,

$$\frac{\tan(qh)}{\tan(ph)} = -\frac{4k^2 pq}{\left(q^2 - k^2\right)^2}, \quad \text{for symmetric modes}$$

$$\frac{\tan(qh)}{\tan(ph)} = -\frac{\left(q^2 - k^2\right)^2}{4k^2 pq}, \quad \text{for anti-symmetric modes}$$

where, $p^2 = \frac{w^2}{c_L^2} - k^2$ and $q^2 = \frac{w^2}{c_T^2} - k^2$

h is half plate thickness, w is circular frequency of vibration, c_L, c_T are longitudinal and shear wave velocities for the medium and k is wave number. Lamb wave is the group of waves that get reflected from upper and lower surface of plate and recombine into a packet at later length. So, Lamb wave travels with the group velocity. This is the speed with which the energy in Lamb wave propagates. Therefore, group velocity is the characteristic of Lamb waves that mainly depends on frequency of vibration as well as thickness of plate. This dependence gives rise to the dispersive nature of Lamb waves. The graph of group velocities verses different frequency-thickness products is called as dispersion curves. Typical dispersion curves for lowest symmetric and anti-symmetric Lamb wave modes for Aluminium are shown in Fig. 3. It can be seen from dispersion curves that the group velocities change as the frequency-thickness product increases.

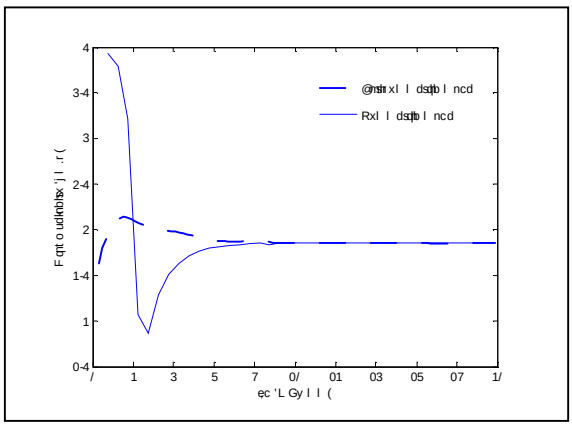

Figure 3: *Dispersion curves for Aluminum*

3. Lamb wave in Finite Difference form

FD methods have been implemented successfully in the field of seismology for elastic waves [13]. In FD methods realistic pulse shapes can be used as an excitation. The output of FD calculations corresponds to the time trace on the oscilloscope of NDE operator. For a plain strain problem equation (1) reduces to

$$u_{tt} = c_T^2(u_{xx} + u_{yy}) + (c_L^2 - c_T^2)(u_{xx} + v_{xy}) \qquad (2)$$

$$v_{tt} = c_T^2(v_{xx} + v_{yy}) + (c_L^2 - c_T^2)(u_{xy} + v_{yy}) \qquad (3)$$

where

$$\frac{\partial^2 u}{\partial x^2} = u_{xx} \qquad \frac{\partial^2 u}{\partial y^2} = u_{yy} \qquad \frac{\partial^2 u}{\partial t^2} = u_{tt} \qquad (4)$$

Similar conventions are used for v. The longitudinal wave speed and shear wave speed is given by,

$$c_L^2 = \frac{l + 2m}{r} \qquad c_T^2 = \frac{m}{r} \qquad (5)$$

u and v are defined over uniform Cartesian mesh of interval h in both x and y directions and at time intervals Δt . In x-y plane u and v can be defined as

$$u(m, n, l) = u(mh, nh, l\Delta t) \qquad (6)$$

and a similar relation for v.

According to second order difference form u can be expressed as

$$u_{tt}(m,n,l)=\frac{1}{\Delta t^2}[u(m,n,l+1)-2u(m,n,l)+u(m,n,l-1)] \quad (7)$$

$$u_{xx}(m,n,l)=\frac{1}{h^2}[u(m+1,n,l)-2u(m,n,l)+u(m-1,n,l)] \quad (8)$$

$$u_{xy}(m,n,l)=\frac{1}{4h^2}\begin{bmatrix}u(m+1,n+1,l)-u(m+1,n-1,l)\\-u(m-1,n+1,l)+u(m-1,n-1,l)\end{bmatrix} \quad (9)$$

Substituting these equations in equations (2 and 3) and defining $\frac{\Delta t}{h}=b$ we get

$$\begin{aligned}&u(m,n,l+1)=2u(m,n,l)(1-b^2c_L^2+b^2c_T^2)\\&-u(m,n,l-1)+b^2c_L^2(u(m+1,n,l)+u(m-1,n,l))\\&+b^2c_T^2(u(m,n+1,l)+u(m,n-1,l))\\&+\frac{b^2(c_L^2-c_T^2)}{4}(v(m+1,n+1,l)-v(m+1,n-1,l)\\&-v(m-1,n+1,l)+v(m-1,n-1,l))\end{aligned} \quad (10)$$

Similar relations can be written for v.
The above system was investigated by Alterman [14], where he gave following stability condition

$$\beta \le 1/\sqrt{(c_L^2+c_T^2)} \quad (11)$$

Condition of stability states that the signal will not be able to propagate across one mesh spacing in less than one time step. Matlab code is developed for FD algorithm. In the code u and v are defined as three dimensional matrix u (M, N, l). M is the number of grid points on x-axis and N is the number of grid points on y-axis. At each grid point, at the beginning of time step $l\Delta t$, the displacements at times $(l-1)\Delta t$ and $(l-2)\Delta t$ are known and the displacements at time $l\Delta t$ are calculated using relations for u and v.

3.1. Boundary conditions

Fundamental difference between bulk wave and Lamb wave is that Lamb wave satisfies stress free boundary condition at top and bottom surface of plate. For stress-free boundaries, the finite difference equations are expressed in one-sided form for derivatives normal to the boundary and in centered form for tangential derivatives [12,13]. This method gave a stability condition in code, which is simple to implement. The application of the method gives the "pseudo node" formulation, in which a row of points is added just outside the free surface, and the displacements of those points are adjusted to give zero stress at the boundaries.

Stress free boundary condition is given as

$$\begin{aligned}&(c_L^2-2c_T^2)u_x+c_L^2v_y=\frac{s_{yy}}{r}=0\\&c_T^2(v_x+u_y)=\frac{s_{xy}}{r}=0\end{aligned} \quad (12)$$

The governing equations for evaluating displacements u and v at points on the boundary are given as

$$\begin{aligned}&(c_L^2-2c_T^2)[u(m+1,n,2)-u(m-1,n,2)]\\&+2c_L^2[v(m,n,2)-v(m,n-1,2)]=0\\&2[u(m,n,2)-u(m,n-1,2)]\\&+v(m+1,n,2)-v(m-1,n,2)=0\end{aligned} \quad (13)$$

Other boundary conditions are evaluated as given in Harker [12].

3.2. Input parameters for simulation

Simulation is done for Aluminum plate for thickness (d in Fig. 4) 3.4 mm and 8 mm. The material properties for Aluminum $c_L = 6230$ m/s and $c_T = 3130$ are taken from Rose [2]. The grid size is chosen as 0.2 mm and time step 0.02 ms. Detector (point R) is moved over plate to detect the signal at various distances.

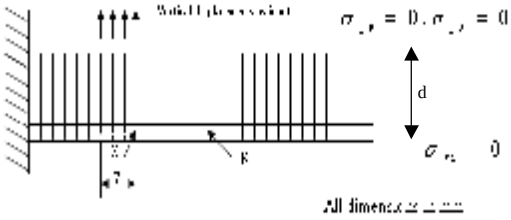

Figure 4: *Simulation Model*

Input normal disturbances are given over 7 mm length and across the thickness of plate in form of tone burst represented by following relation as given in reference [15].

$$u(t)=\begin{cases}u_0\sin(wt).\left\{\sin(\frac{wt}{10})\right\}^2 & t<\frac{10p}{w}\\0 & otherwise\end{cases} \quad (14)$$

Simulation results are presented as time history. A time history is the graph of the displacement of a particular point on the grid as a function of time. This corresponds to an experimental signal taken by oscilloscope

4. Experimental Details

The Laser based ultrasonic (LBU) setup consists of an Nd: YAG pulsed laser to generate ultrasonic Lamb waves and a Heterodyne laser interferometer to detect the transmitted acoustic signal through the material. The set-up utilizes a Yokogawa DL1740 (four channel, one GSa/sec, 500 MHz) Digital Storage Oscilloscope. The schematic layout is shown in Fig. 5. The scanning is done manually using an XY translator mounted on an Optical Test Bench.

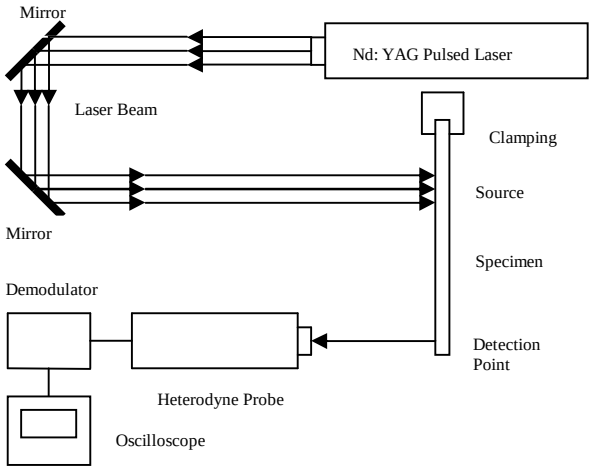

Figure 5: *Schematic of experimental set-up*

Two Aluminium plates of thickness 3.4 mm and 8 mm are used as a specimen to generate Lamb waves. The laser power is kept at 200 mJ. A precise calibration of heterodyne interferometer is done prior to the experiment. Wavelet transforms are obtained using Morlet mother wavelet. These wavelet transforms are compared with the wavelet transform of simulated signals. The arrival times of different frequency components are extracted from the wavelet transforms. Knowing the arrival times, group velocities at a particular frequency are calculated and the values are compared with those obtained from the simulation.

5. Results and Discussion

As the recorded signals are expected to contain various frequencies, the wavelet transform of each signal is used to analyze the arrival time for different frequencies. The fundamental idea behind wavelets is to analyze according to scale. Wavelet transform of signal obtained for 8mm plate (Figs. 6 and 7) shows 3 windows. Window at the top shows the signal whose wavelet is to be taken. Middle window shows the three-dimensional plot in which x-axis corresponds to time, y-axis corresponds to frequency according to scale, and z-axis shows the variation of amplitude. The variation in amplitude is depicted in the Figs. (6 and 7) with the help of different colors with red corresponding to maximum intensity. Last window gives temporal distribution of signal at frequency corresponding to a given scale.

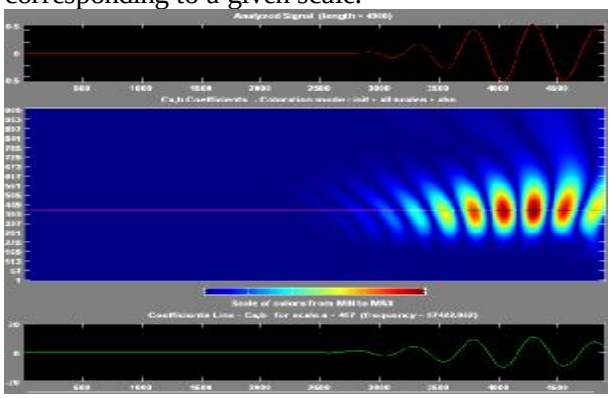

Figure 6: *Wavelet transform of signal of 8mm plate at 200 mm separation (Simulated)*

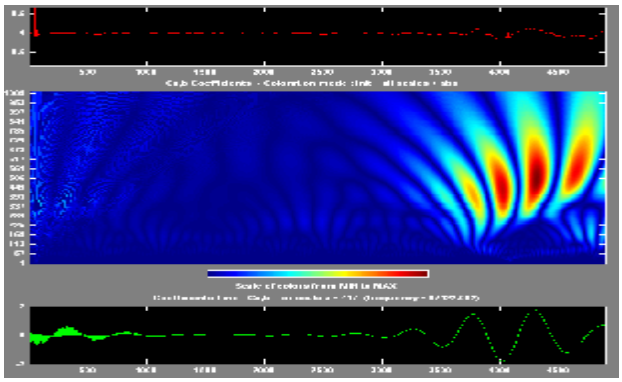

Figure 7: *Wavelet transform of signal of 8 mm plate at 200 mm separation (Experimental)*

From both the wavelets (Figs. 6 and 7) one can notice the experimental signal contains the intensity (color) distribution same as that of the output signal from simulation when a tone burst is used as input in the simulation. According to Harker [12], when normal stress is given as input to plate the symmetric modes will have less probability of generation. As the generation of waves is through normal disturbances in experimental condition, only A_0 mode is obtained with greater intensity. In simulation also the normal displacements are given as input to plate over 7 mm length and a sampling period of 20 ns is used for the evaluation of both wavelet transforms. The mother wavelet used is Morlet whose center frequency is 0.8125 Hz. From Figs. 6 and 7, the arrival time for A_0 mode for source to detector distance of 200 mm by simulation is coming out to be $62\,ms$ and by experiments it is coming out to be $68\,ms$ at 97 kHz. The velocity by simulation is 3.22 km/s and by experiment it is coming out to be

2.94 km/s. The velocity for A_0 mode from dispersion curve is 3.06 km/s. The coefficients of wavelets are stored in matrix form for further analysis.

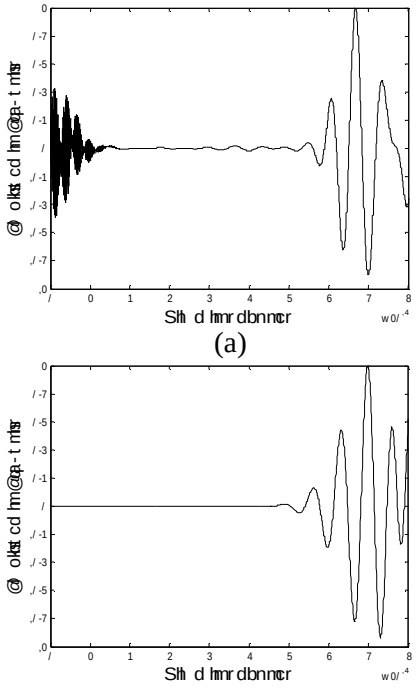

(a)

(b)

Figure 8: (a) *Experimental Signal* (b) *Simulated Signal at 253 kHz obtained from wavelet transform (source to detector distance 200 mm, plate thickness 8mm)*

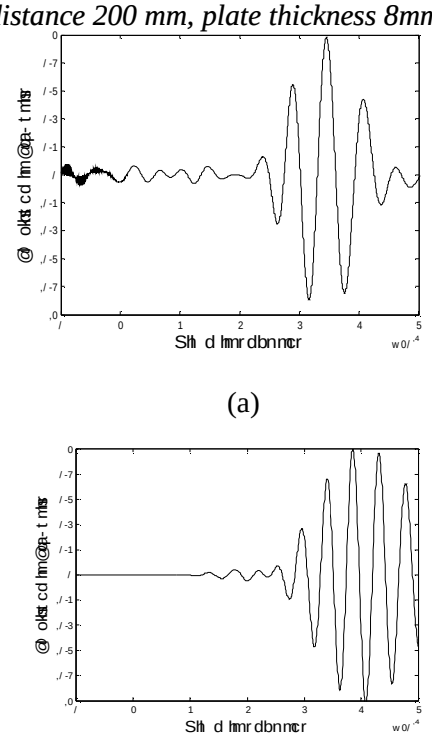

(a)

(b)

Figure 9**:** (a) *Experimental Signal* (b) *Simulated Signal at 203 kHz obtained from wavelet transform (source to detector distance, 85mm, plate thickness 3.4 mm)*

At a particular point on the y-axis i.e. when the scale fixed, the plot between x and z-*axes* will give temporal distribution of the signal at particular frequency. The experimental and simulated signals obtained from wavelet transforms at 253 kHz for 8mm plate and at 203 kHz for 3.4mm plate are shown in Figs. 8 and 9 respectively. The disturbances seen near zero microseconds in Figs. 8(a) and 9(a) are due to trigger characteristic of the laser pulse.

Table 1: Comparison between experimental and simulation result

Frequency-thickness (*fd*) (MHz-mm)	Group velocity of A_0 mode by simulation (km/s)	Group velocity of A_0 mode by experiment (km/s)
2.024	3.22	2.94
0.692	2.42	2.65

In Fig. 9 the presence of S_0 mode can be seen preceding A_0 mode with smaller amplitude as expected. Table 1 shows the comparison between group velocities obtained from experiments and simulation. The results are evidently in good agreement.

5.1 Dependence of mode amplitude on frequency

From Fig. 10 shows the time history of the signal obtained from the wavelet transform of the experimental signal on 3.4 mm plate with source-detector separation of 85mm. In this figure both S_0 and A_0 modes can be seen to appear simultaneously. These modes are identified with the help of their group velocities

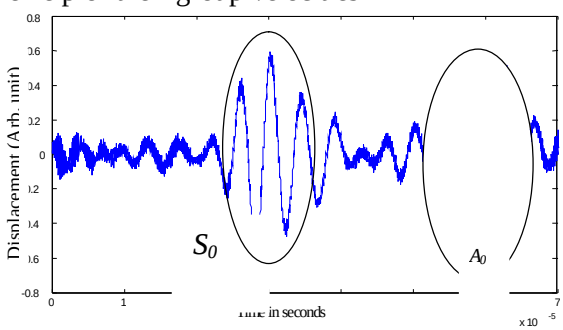

Figure 10: *Time history of signal at 251 KHz on 3.4 mm plate(experimental).*

Figure 11 shows result of FEM simulation done by Nieuwenhuis[15]. The encircled region shows the matching between the amplitudes of two modes at frequency of 250 kHz

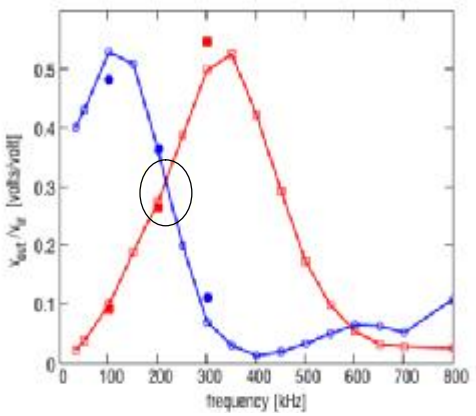

Figure 11: *Simulated results for dependence of mode amplitude on excitation frequency [15*].

Figure 12 (a and b) shows the temporal distribution (obtained by wavelet) of the experimental results conducted on 3.4 mm thick plate at source-detector separation distance of 85mm. One can obviously see the amplitude of the S_0 mode to be equal to that of A_0 mode around 250 kHz while it is much less at 120 kHz in agreement with the results shown in Fig. 11

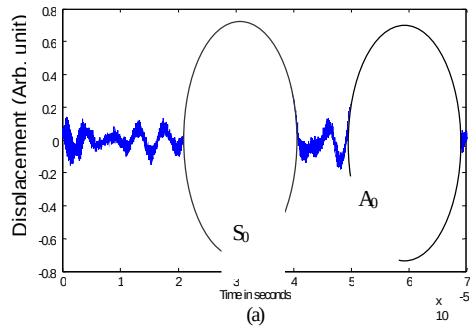

Figure 12: *Signals at separation distance 85 mm (a) at 231 kHz, (b) at 120 kHz.*

Conclusions:

In the present work the results of FDM simulation of Lamb waves in Aluminium plates of different thickness and their correlation with Laser generated lamb waves are presented. Wavelet Transforms are used to study this correlation. The work presented in this paper clearly brings out the utility of wavelet transforms in the analysis of complex signals as well as in confirming the accuracy of any simulation work. The variation of amplitude of different Lamb wave modes with frequency is studied with the help of wavelet transforms of the experimental signals and a good correlation between the experimental and simulation results is observed.

6 References:

[1] Viktorov I. A, *Rayleigh and Lamb wave. Physical Theory and Applications,*: Plenum, New York 1970.

[2] Rose, J. L, *Ultrasonic waves in solid media*, The Pennsylvania State University, Cambridge University Press, 1999.

[3] Graff, K.F., *Wave Motions in Elastic Solids*, Dover Publications Inc., 1991.

[4] Achenbach J. D. *Wave propagation in elastic solids*, North Holland publishing company,1973.

[5] Alleyene, D. N, Cawley, P., "The interaction of lamb waves with defects*", IEEE Trans. Ultrason. Ferroelectr. Freq. Control*, 39 (3) 381-97, 1992

[6] Worlton D. C. Ultrasonic testing with Lamb waves *Non-dest. Testing,(*15) 218–22, 1957.

[7] Cheng J. C., "Theory of laser-generated transient Lamb waves in orthotropic plates", *J. Phys. D: Appl. Phys.*, (29) 1857-67, 1996.

[8] Tan K. S., Guo N., Wong B. S., "Experimental evaluation of delaminations in composite plates by the use of Lamb waves", *Composite Science and Technology*, 53 (2) 404-11, 1994.

[9] Bertholf L. D., "Numerical solutions to two-dimensional elastic wave propagation in finite bars", *J. Appl. Mech. (*34) 725–734, 1967.

[10] Alterman Z., "Finite difference solutions to geophysical problems" *J. Phys. Earth,* (16) 113–128, 1968.

[11] Balasubramanyamy R., Quinneyz D., Challisy R E and Toddy, C. P. D., "A finite-difference simulation of ultrasonic Lamb waves in metal sheets with experimental verification", *J. Phys. D: Appl. Phys.* (29) 147–155, 1996.

[12] Harker A. H., "Numerical modelling of the scattering elastic waves in plates", *J. Non-dest. Eval.* (4) 89–106, 1984.

[13] Alterman, Z. S, and Loewenthal, D, "Seismic waves in a quarter and three quarter plane" *Geophys. J. Roy. Astron. Soc, (*20):101,1970.

[14] Alterman, Z, and Loewenthal, D., "Computer generated seismograms", *Methods in Computational Physics, V*ol 12, ed Adder, B *et al.,*: Academic Press, New York, 1972

[15] Nieuwenhuis J.H., Neumann J. J., Greve D.W., and Oppenheim I.J. ''Simulation and Testing of Transducers for Lamb wave Generation." *IMAC-XXIII Conference on Structural Dynamics, Society for Experimental Mechanics, Orlando, February 2005.*